Stimulated Raman adiabatic passage through permanent dipole moment transitions

Ying-Yu Niu,* Rong Wang, and Ming-Hui Qiu
School of Science, Dalian Jiaotong University, Dalian 116028, People's Republic of China
(Received 18 January 2010; published 12 April 2010)

The rovibrational dynamics of stimulated Raman adiabatic passage (STIRAP) through permanent dipole moment transitions are investigated theoretically using a time-dependent quantum wave packet method for the ground electronic state of an HF molecule. The two basic STIRAP processes, Λ and ladder systems, are simulated. The calculated results show that nearly 100% of the population can be transferred to the target state. Besides the interested transitions, the pulses can induce other transitions which affect the dynamics of STIRAP. The final populations of the initial and target states depend on delay time.

DOI: 10.1103/PhysRevA.81.043406 PACS number(s): 33.80.Be, 42.65.Dr, 33.20.Fb

I. INTRODUCTION

In recent years, the interaction of molecules with the laser field is an interesting and active research subject [1–3]. Many investigations have been focused on the preparation of well-defined quantum states by properly designed laser fields [4–6]. The manipulation of population to a prescribed target state is relevant to many applications, including optical control of chemical reactions, molecular spectroscopy, and collision dynamics. Several approaches have been proposed to control population transfer, such as optimal control theory (OCT) [7,8], multipath interference [9], chirped laser pulse [5,10], or adiabatic passage [11–13].

Stimulated Raman adiabatic passage (STIRAP) technique has become an important tool for controlling population transfer in both atomic and molecular systems [14–18]. The STIRAP method employs two partly overlapping laser pulses in which the Stokes pulse precedes the pump pulse. In its simplest three-level system, the initial state $|1\rangle$ is coupled with intermediate state $|2\rangle$ by a pump pulse, state $|2\rangle$ is coupled with target state $|3\rangle$ by a Stokes pulse. This two-pulse scheme can produce a complete population transfer from states $|1\rangle$ to $|3\rangle$ without a significant population in state $|2\rangle$. According to the energy distribution of the three states, the STIRAP process is divided into Λ and ladder systems. Many investigations about these two systems have been reported in detail both theoretically and experimentally [19–23]. In most cases, the three-level system is composed of two or three bound electronic states, and the population transfer takes place in different bound electronic states through dipole moment transitions [24–26].

In this article, we take the HF molecule for example to explore the rovibrational dynamics of STIRAP in a ground electronic state using the time-dependent quantum wave packet method. For the ground electronic state of an HF molecule, the adjacent electronic state is not suitable for the intermediate state because of a large energy gap (more than 14 eV) at the equilibrium distance. In our model, the three-level system is described by the three rovibrational levels in the ground electronic state, and the STIRAP process is achieved by permanent dipole moment transitions. We numerically investigate the transition ($|0,0\rangle \rightarrow |2,1\rangle \rightarrow |1,0\rangle$) for the Λ system, and the transition ($|0,0\rangle \rightarrow |1,1\rangle \rightarrow |3,0\rangle$) for the ladder system, as shown in Fig. 1. The two counterintuitive pulses can induce a nearly complete population transfer from the initial state to the target state via the intermediate state.

This article is organized as follows: In Sec. II we introduce the time-dependent wave packet method that we use for dynamics calculation of population transfer. In Sec. III. we calculate the populations of the three rovibrational levels, and discuss the effect of the delay time on the population transfer. Finally, some conclusions are briefly summarized in Sec. IV.

II. THEORETICAL METHOD

In our model, the ground electronic state of an HF molecule is taken into account. In the Born-Oppenheimer approximation, the wave function $\Psi(t)$ is obtained by solving the time-dependent Schrödinger equation

$$i\hbar\frac{\partial}{\partial t}\Psi(t) = [\hat{H}_{\rm mol} + \hat{W}]\Psi(t), \tag{1}$$

where $\hat{H}_{\rm mol}$ is the time-independent Hamiltonian of the HF molecule. In the present work, we assume the initial rovibrational level to be $|\nu = 0, j = 0\rangle$. In the linearly polarized laser field, the molecular magnetic quantum number $m = 0$ is conserved, and the two-dimensional molecular Hamiltonian can be expressed as

$$\begin{aligned}\hat{H}_{\rm mol}(R,\theta,t) &= \hat{T}_R + \hat{T}_\theta + \hat{V} \\ &= -\frac{\hbar^2}{2m}\frac{\partial^2}{\partial R^2} - \frac{\hbar^2}{2mR^2}\frac{1}{\sin\theta}\frac{\partial}{\partial\theta}\left(\sin\theta\frac{\partial}{\partial\theta}\right) \\ &\quad + \hat{V}(R),\end{aligned} \tag{2}$$

where m is the reduced mass of the two nuclei, R the internuclear separation, and θ the angle between the molecular axis and the laser electric field axis. $V(R)$ stands for the Morse potential function

$$V(R) = D_0\{\exp[-2\beta(R-R_0)] - 2\exp[-\beta(R-R_0)]\}, \tag{3}$$

where the equilibrium distance $R_0 = 1.732516\ a_0$, Morse parameter $\beta = 1.174014\ a_0^{-1}$ (a_0 is the Bohr radius), and

*niuyy@djtu.edu.cn

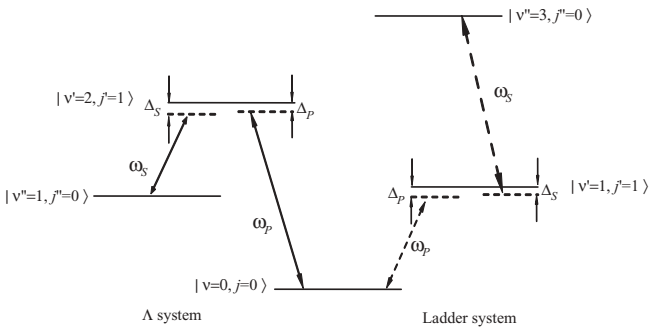

FIG. 1. Schematic diagram of the three-level Λ and ladder systems.

well depth $D_0 = 0.225009$ hartree [27]. In the dipole approximation, the field-molecule interaction term $\hat{W}$ can be written as

$$\hat{W} = -\mu(R)\cos\theta\varepsilon(t), \tag{4}$$

with

$$\mu(R) = \mu_0 R\exp(-\xi R^4), \tag{5}$$

with parameters $\mu_0 = 0.454141\ e$ and $\xi = 0.0064\ a_0^{-4}$ [27]. The electric field $\varepsilon(t)$ of the two laser pulses is given by

$$\begin{aligned}\varepsilon(t) &= \varepsilon_P(t) + \varepsilon_S(t)\\ &= E_P\sin^2\left[\frac{\pi(t-t_P)}{\tau_P}\right]\cos(\omega_P t)\\ &\quad + E_S\sin^2\left[\frac{\pi(t-t_S)}{\tau_S}\right]\cos(\omega_S t),\end{aligned} \tag{6}$$

where $t_{P(S)}$, $E_{P(S)}$, $\omega_{P(S)}$, and $\tau_{P(S)}$ are the start time, electric field amplitude, carrier frequency, and duration of the two pulses, respectively. $t'_{P(S)} = t_{P(S)} + \tau_{P(S)}/2$ is the center time of the pulses. The delay time between the two laser pulses can be obtained by $\Delta t = t'_S - t'_P$.

The initial wave function is described by the rovibrational eigenfunction $|\nu = 0,\ j = 0\rangle$. The rovibrational eigenfunction $|\nu,\ j\rangle$ can be obtained by a direct product of radial eigenfunction $\phi_{\nu,j}(R)$ and the Legendre polynomial $P_j(\cos\theta)$, which is the eigenfunction of the angular part [28]. The j-dependent vibrational function $\phi_{\nu,j}(R)$ and the rovibrational eigenvalue $E_{\nu,j}$ can be solved by the Fourier grid Hamiltonian method [29]. The initial wave function is propagated using the split operator method [30], that is,

$$\begin{aligned}\Psi(t+\Delta t) &= e^{-i\Delta t\left[\hat{T}_R+\hat{T}_\theta+\hat{V}(R)+\hat{W}(R,\theta)\right]/\hbar}\Psi(t)\\ &\approx e^{-i\Delta t\hat{T}_R/2\hbar}e^{-i\Delta t\hat{T}_\theta/2\hbar}e^{-i\Delta t\left[\hat{V}(R)+\hat{W}(R,\theta)\right]/\hbar}\\ &\quad\times e^{-i\Delta t\hat{T}_\theta/2\hbar}e^{-i\Delta t\hat{T}_R/2\hbar}\Psi(t).\end{aligned} \tag{7}$$

In the calculation, the fast Fourier transform method [31] is employed to solve operator $\hat{T}_R$ by transforming Ψ between momentum space and coordinate space. Using the discrete variable representation technique [32], Ψ is switched forward and backward between the polynomial representation and the coordinate space to calculate operator $\hat{T}_\theta$. The operators $\hat{V}(R)$ and $\hat{W}(R,\theta)$ act on the wave function directly in the coordinate space by multiplication.

The time-dependent populations $P_{\nu,j}$ of the rovibrational levels are calculated by the projection of wave function on rovibrational eigenstates

$$P_{\nu,j}(t) = |\langle\nu,\ j|\Psi(t)\rangle|^2. \tag{8}$$

The time-dependent vibrational and rotational energies of the wave function are computed by

$$\begin{aligned}E'_{\rm tot}(t) &= \langle\Psi(t)|\hat{T}_R + \hat{T}_\theta + \hat{V}|\Psi(t)\rangle\\ &= \langle\Psi(t)|\hat{T}_R + \hat{V}|\Psi(t)\rangle + \langle\Psi(t)|\hat{T}_\theta|\Psi(t)\rangle\\ &= E'_\nu + E'_j,\end{aligned} \tag{9}$$

where E'_ν and E'_j are the vibrational and rotational energies of the wave function, respectively.

III. RESULTS AND DISCUSSION

A. STIRAP in a Λ system

We focus on the specific example of a Λ system (see Fig. 1) in which the initial rovibrational state is $|\nu = 0,\ j = 0\rangle$, the intermediate state $|\nu' = 2,\ j' = 1\rangle$, and the target state $|\nu'' = 1,\ j'' = 0\rangle$. In this transition process, $\Delta j = j'' - j = 0$ corresponds the Q branch of the Ramam transition.

Figure 2 shows the nearly complete population transfer from the initial state to the target state. The left and right-hand panels are obtained within the intuitive pulse sequence and the counterintuitive pulse sequence. From Fig. 2, we can see that the durations and amplitudes in Fig. 2(e) are larger than those in Fig. 2(b). In Fig. 2(a), the population transfers from $|0,0\rangle$ to $|2,1\rangle$ induced by the pump pulse, and then to $|1,0\rangle$ induced by the Stokes pulse. The final populations of the intermediate and target states at the end of the respective pulse are 0.999 and 0.991. The oscillatory behavior of the curve demonstrates that little population transfers to other bound states during the transition from $|0,0\rangle$ to $|2,1\rangle$. In Fig. 2(d), the population $P_{0,0}$ decreases, and the population $P_{1,0}$ increases induced by the two pulses. A small amount of population $P_{2,1}$ ($<10\%$) can be found in the intermediate state during the laser-molecule interaction. When the pump pulse is over, the final populations $P_{0,0}$, $P_{2,1}$, and $P_{1,0}$ reach 0.001, 0.013, and 0.981, respectively. Besides the previous two transitions, the two partly overlapping pulses can produce other excitation pathways, such as $|0,0\rangle \rightleftarrows |1,1\rangle \rightleftarrows |2,0\rangle \rightleftarrows |0,1\rangle$ and $|0,0\rangle \rightleftarrows |1,1\rangle \rightleftarrows |2,2\rangle \rightleftarrows |0,1\rangle$. Therefore, the curves of the populations display obvious oscillatory behavior. Figures 2(c) and 2(f) show the time-dependent energy of the wave function. In Fig. 2(c), the energy increases from -0.2157 a.u. to -0.1802 a.u., which corresponds to the revibrational eigenenergy of the state $|\nu' = 2,\ j' = 1\rangle$, and then decreases to -0.1977 a.u., which corresponds to the revibrational eigenenergy of the state $|\nu'' = 1,\ j'' = 0\rangle$. It can be seen from Fig. 2(e) that the energy of the wave function increases from -0.2157 a.u. to -0.1977 a.u. directly. This indicates that the population in the state $|\nu' = 2,\ j' = 1\rangle$ is very small during the whole transition process.

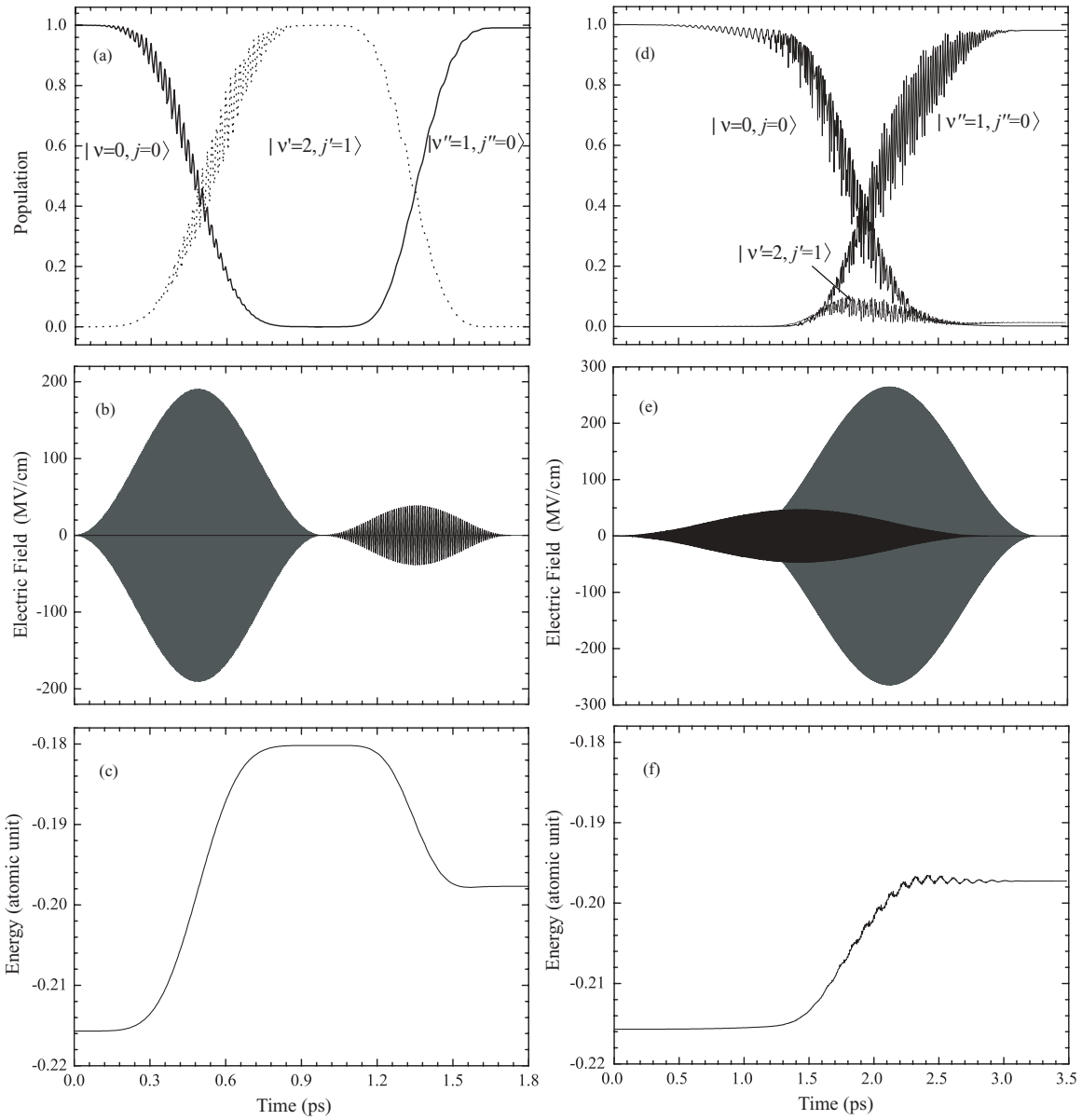

FIG. 2. Complete population transfer from the initial state $|\nu = 0, j = 0\rangle$ to the target state $|\nu'' = 1, j'' = 0\rangle$ via the intermediate state $|\nu' = 2, j' = 1\rangle$. Results obtained within the intuitive pulse sequence (left-hand panels) and the counterintuitive pulse sequence (right-hand panels) are compared. (a) and (d) Population dynamics. (b) The pump and Stokes pulses with a intuitive sequence: $E_P = 190.52$ MV/cm, $\omega_P = 7795.83$ cm^{-1}, $\tau_P = 0.98$ ps, $t'_P = 0.49$ ps, $E_S = 38.57$ MV/cm, $\omega_S = 3829.39$ cm^{-1}, $\tau_S = 0.75$ ps, $t'_S = 1.35$ ps. (e) The pump and Stokes pulses with a counterintuitive sequence: $E_P = 264.57$ MV/cm, $\omega_P = 7783.32$ cm^{-1}, $\tau_P = 2.27$ ps, $t'_P = 2.13$ ps, $E_S = 46.80$ MV/cm, $\omega_S = 3810.74$ cm^{-1}, $\tau_S = 2.88$ ps, $t'_S = 1.44$ ps. (c) and (f) Time-dependent energy of the wave function.

In Fig. 2(e), the frequencies of the pump and Stokes pulses are 7783.32 cm^{-1} and 3810.74 cm^{-1}, and the one-photon detunings of the two pulses from their transition frequencies are $\Delta_P = -11.64\,\text{cm}^{-1}$ and $\Delta_S = -19.32\,\text{cm}^{-1}$, respectively. Figure 3(a) shows the final rovibrational populations in the states $|0, 0\rangle$, $|1, 0\rangle$, and $|2, 1\rangle$ with two-photon detuning $\Delta = 0$, where the frequency of the Stokes pulse is $3818.42\,\text{cm}^{-1}$, and the other laser pulse parameters are the same as those in Fig. 2(e). From Fig. 3(a), we find that the population $P_{0,0}$ decreases when $t < 2.3$ ps, and then increases when $t > 2.3$ ps. The final populations of the initial and target states are 0.111 and 0.868, respectively. Usually, the most efficient population transfer can be obtained as the two-photon resonance $\Delta = |\Delta_S| - |\Delta_P| = 0$ is met in the STIRAP thought dipole moment transitions. However, in this case, the population transfer with the two-photon detuning $\Delta = 7.68\,\text{cm}^{-1}$ is more efficient than that with the detuning $\Delta = 0$. In our model, the population transfer takes place in the ground electronic state through permanent dipole moment transitions, and the energy gap of the three levels is small, which results in other transitions. Figures 3(b) and 3(d) show the time-dependent populations in the states $|2, 0\rangle$ and $|2, 2\rangle$

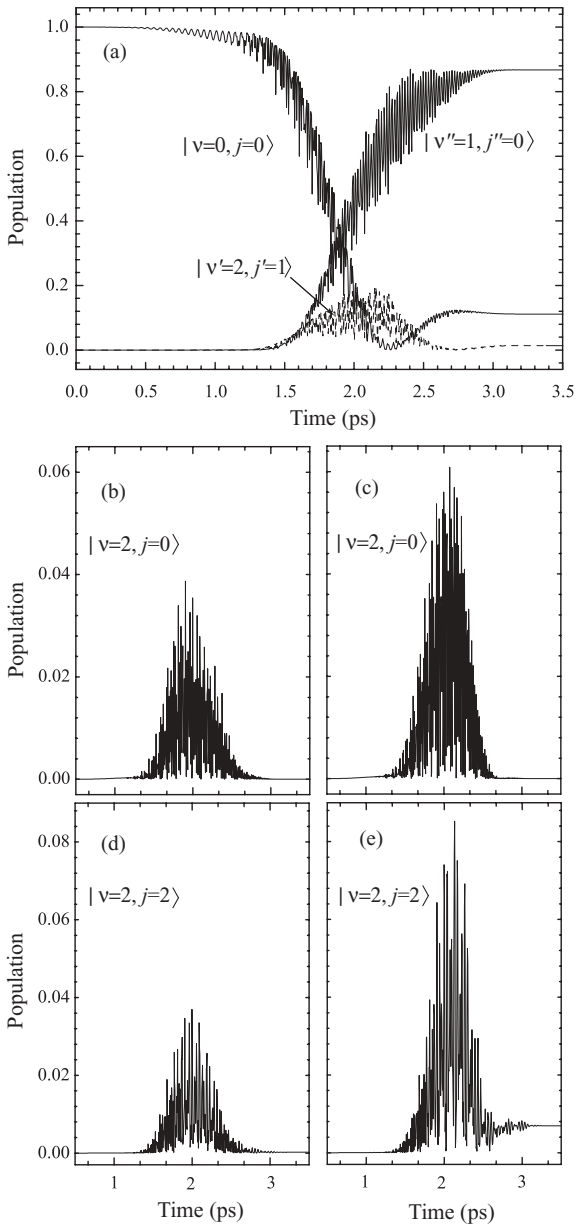

FIG. 3. (a) The time-dependent populations in the revibrational states $|0,0\rangle$, $|1,0\rangle$, and $|2,1\rangle$ with two-photon detuning $\Delta = |\Delta_S| - |\Delta_P| = 0\,\mathrm{cm}^{-1}$. (b) and (d) The time-dependent populations in the states $|2,0\rangle$ and $|2,2\rangle$ with two-photon detuning $\Delta = 7.68\,\mathrm{cm}^{-1}$. (c) and (e) The time-dependent populations in the states $|2,0\rangle$ and $|2,2\rangle$ with two-photon detuning $\Delta = 0\,\mathrm{cm}^{-1}$.

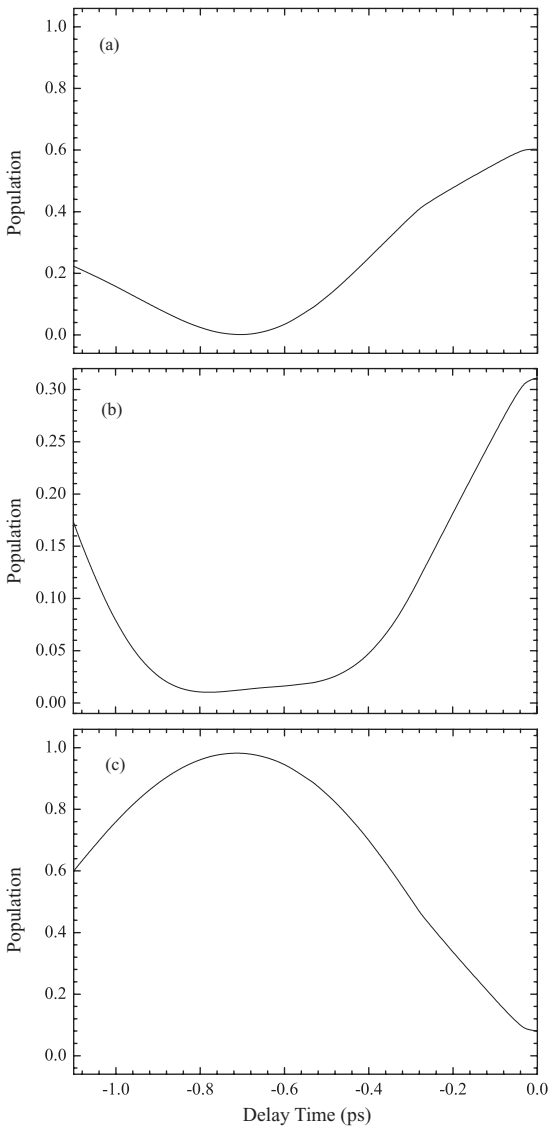

FIG. 4. The final populations at the end of the pulse sequence versus the delay time Δt. (a) The population of the initial state. (b) The population of the intermediate state. (c) The population of the target state. All other parameters are the same as in Fig. 2(e).

as two-photon detuning $\Delta = 7.68\ \mathrm{cm}^{-1}$. The Stokes pulse can induce the population $P_{0,0}$ to transfer to $|1,1\rangle$, and then to $|2,0\rangle$ or to $|2,2\rangle$. The one-photon detunings for the three transitions are $-194.07\,\mathrm{cm}^{-1}$, $59.14\,\mathrm{cm}^{-1}$, and $56.47\,\mathrm{cm}^{-1}$, respectively. The large amplitude oscillations of the curves in Figs. 2(b) and 2(d) illustrate that the population transfer to and fro takes place in the states $|0,0\rangle$, $|1,1\rangle$, $|2,0\rangle$, and $|2,2\rangle$. We can see that the populations $P_{2,0}$ and $P_{2,2}$ increase to the maximal value at $t = 2.0$ ps, and then decrease to 0 at $t = 3.5$ ps. This indicates that all the populations in the states $|2,0\rangle$ and $|2,2\rangle$ have been transferred back to $|0,0\rangle$ because of the large detunings. It can be seen from Fig. 2(d) that almost all of the population $P_{0,0}$ derived from $|2,0\rangle$ and $|2,2\rangle$ can be transferred to $|1,0\rangle$ through the STIRAP process. When $\omega_S = 3818.42\ \mathrm{cm}^{-1}$ in Figs. 3(c) and 3(e), the detuning of the transition $|0,0\rangle \rightleftarrows |1,1\rangle$ is reduced, and the populations $P_{2,0}$ and $P_{2,2}$ are increased. As these increased populations transfer back to $|0,0\rangle$, only part of population $P_{0,0}$ can be transferred to $|1,0\rangle$ through the STIRAP process, and some population (about 11%) can be found in the state $|0,0\rangle$.

The populations of the three states depend on the parameters of the two pulses. Figure 4 shows the final populations versus the delay time Δt. As the delay time of the two pulses increases from -1.1 to -0.69 ps in Fig. 4, the final populations $P_{0,0}$ and $P_{2,1}$ decrease, and $P_{1,0}$ increases. As the delay time Δt increases from -0.69 to 0 ps, the final populations $P_{0,0}$ and $P_{2,1}$ increase, and $P_{1,0}$ decreases.

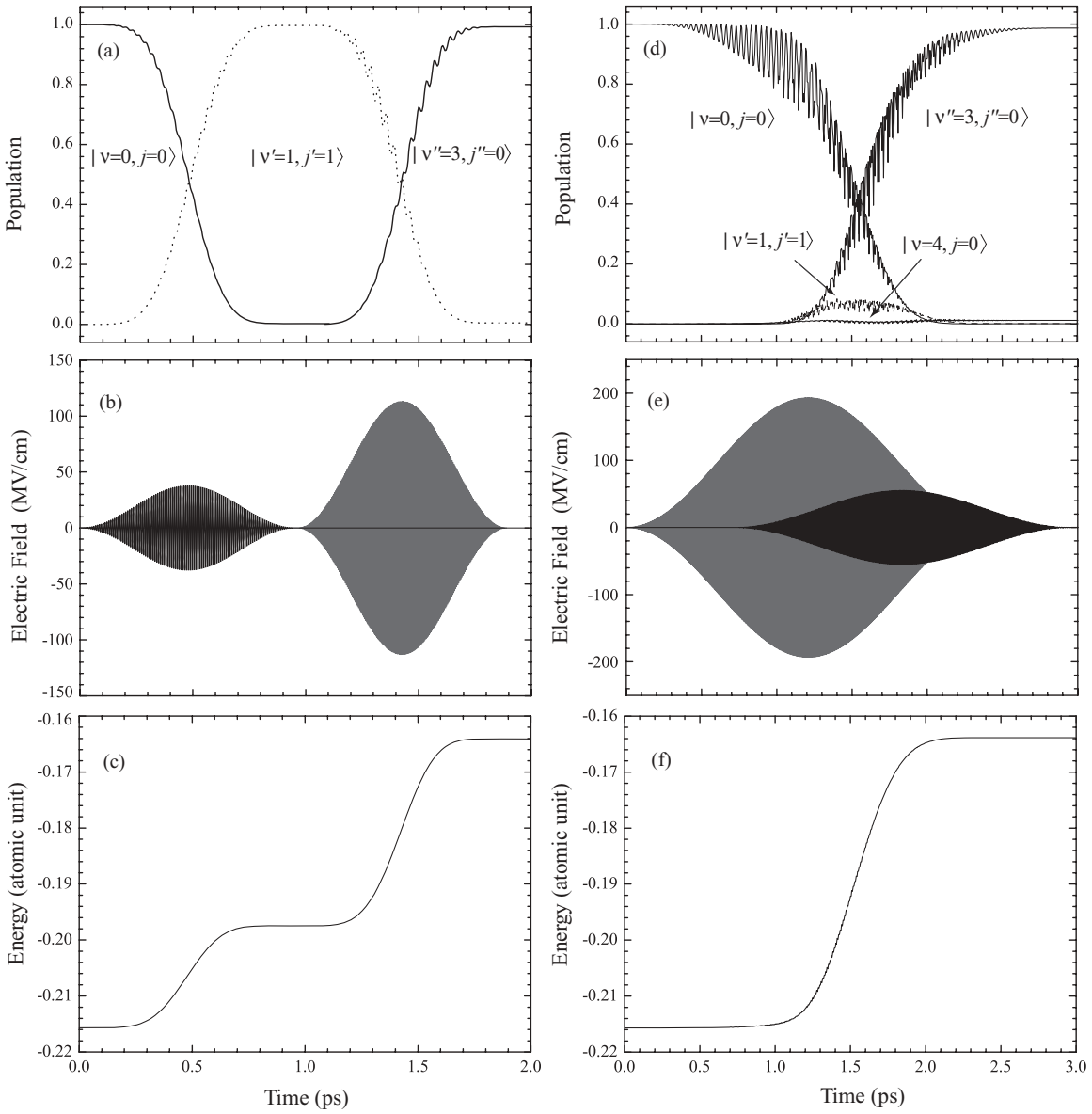

FIG. 5. Complete population transfer from the initial state $|\nu = 0, j = 0\rangle$ to the target state $|\nu'' = 3, j'' = 0\rangle$ via the intermediate state $|\nu' = 1, j' = 1\rangle$. Results obtained within the intuitive pulse sequence (left-hand panels) and the counterintuitive pulse sequence (right-hand panels) are compared. (a) and (d) Population dynamics. (b) The pump and Stokes pulses with a intuitive sequence: $E_P = 37.80$ MV/cm, $\omega_P = 4005.46$ cm^{-1}, $\tau_P = 0.96$ ps, $t'_P = 0.48$ ps, $E_S = 113.13$ MV/cm, $\omega_S = 7370.57$ cm^{-1}, $\tau_S = 0.93$ ps, $t'_S = 1.43$ ps. (e) The pump and Stokes pulses with a counterintuitive sequence: $E_P = 55.28$ MV/cm, $\omega_P = 3975.17$ cm^{-1}, $\tau_P = 2.23$ ps, $t'_P = 1.84$ ps, $E_S = 193.35$ MV/cm, $\omega_S = 7396.27$ cm^{-1}, $\tau_S = 2.42$ ps, $t'_S = 1.21$ ps. (c) and (f) Time-dependent energy of the wave function.

When $\Delta t = 0$, the final population of the target state is only 0.082.

B. STIRAP in a ladder system

We now consider a ladder process (see Fig. 1) in which the initial state $|\nu = 0, j = 0\rangle$ and intermediate state $|\nu' = 1, j' = 1\rangle$ are coupled by the pump pulse, and $|\nu' = 1, j' = 1\rangle$ is coupled with the target state $|\nu'' = 3, j'' = 0\rangle$ by the Stokes pulse. Figure 5 shows the nearly complete population transfer from the initial state to the target state. The left-hand panels show results obtained within the intuitive pulse sequence, and the right-hand panels are for the counterintuitive pulse sequence. Similarly to the Λ system in Fig. 2, the durations and amplitudes for the counterintuitive pulse sequence in Fig. 5(e) are larger than that for the intuitive pulse sequence in Fig. 5(b). From Fig. 5(d), we can see that 98.7% of the population can be transferred to the target state. For the intermediate state, the population $P_{1,1}$ increases to the maximal value 0.081 at $t = 1.52$ ps, and then decreases to 0.001 at the end of the two pulses. Besides the transition $|1, 1\rangle \rightarrow |3, 0\rangle$, the Stokes pulse can provide the other two transitions, $|0, 0\rangle \rightleftarrows |2, 1\rangle$ and $|2, 1\rangle \rightleftarrows |4, 0\rangle$. Therefore, 1.2% of the population can be transferred to $|4, 0\rangle$ in Fig. 5(d). In Fig. 5(c), the energy of the wave function increases from -0.2157 a.u. to -0.1975 a.u., which corresponds to the revibrational eigenenergy of the

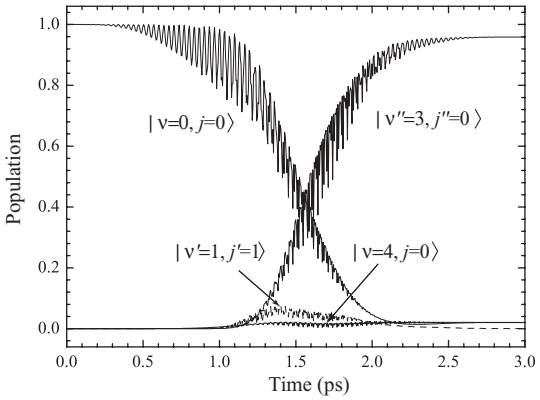

FIG. 6. The time-dependent populations in the revibrational states $|0,0\rangle$, $|1,1\rangle$, $|3,0\rangle$, and $|4,0\rangle$ with two-photon detuning $\Delta = 0\,\mathrm{cm}^{-1}$.

state $|v' = 1, j' = 1\rangle$, and then increases to -0.1641 a.u., which corresponds to the revibrational eigenenergy of the state $|v'' = 3, j'' = 0\rangle$. The increment speed of the energy for the transition $|1,1\rangle \rightarrow |3,0\rangle$ is larger than that for the transition $|0,0\rangle \rightarrow |1,1\rangle$. In Fig. 5(f), the energy directly increases from -0.2157 a.u. to -0.1641 a.u. with a constant speed.

In Fig. 5(e), the one-photon detunings of the pump and Stokes pulses from their respective transition frequencies are $-29.64\,\mathrm{cm}^{-1}$ and $26.56\,\mathrm{cm}^{-1}$, and the corresponding two-photon detuning is $-3.08\,\mathrm{cm}^{-1}$. Figure 6 shows time-dependent populations with two-photon detuning $\Delta = 0$, where the frequency of the Stokes pulse is 7399.35 cm^{-1}, and the other laser pulse parameters are the same as those in Fig. 5(e). The one-photon detuning of the Stokes pulse for the transition $|0,0\rangle \rightleftarrows |2,1\rangle$ in Fig. 6 is smaller than that in Fig. 5(d). More population can be transferred to $|4,0\rangle$ via $|2,1\rangle$. When the two pulses are over, 2.1% of the population can be found in the state $|4,0\rangle$. Because of the to and fro population transfer in the states $|0,0\rangle$, $|2,1\rangle$, and $|4,0\rangle$, 2% of the population stays in the state $|0,0\rangle$. The final population of the target state is 0.959 at the end of the pulses.

Figure 7 shows the final populations versus the delay time Δt. From Figs. 7(a) and 7(c), we can see that the final populations of the initial and target states are very sensitive to the delay time. When $\Delta t = -0.63$ ps, the final population $P_{0,0}$ reaches the minimal value 0, and $P_{3,0}$ reaches the maximal value 0.987. When $\Delta t = 0$ ps, only 11.0% of the population can be transferred to the target state, and 87.2% of the population stays in the initial state. For the intermediate state in Fig. 7(b), the final population reaches the maximal value 0.017 when the delay time is 0 ps. Comparing with Fig. 4(b), the variation of the delay time has a small effect on the distribution of the final population in Fig. 7(b).

IV. CONCLUSION

In this article, we have studied the rovibrational dynamics of STIRAP through permanent dipole moment transitions in the ground electronic state, with the HF molecule as the example. The two basic STIRAP processes, Λ and ladder systems, are described by the two transitions $|0,0\rangle \rightarrow |2,1\rangle \rightarrow |1,0\rangle$ and $|0,0\rangle \rightarrow |1,1\rangle \rightarrow |3,0\rangle$. The calculated results show that nearly 100% of the population can be transferred to the target state. Besides the interested transitions, we found that the pulses can induce other transitions. Under the condition of the two-photon resonance, the unexpected transitions will be increased, which affects the dynamics of STIRAP. The population distributions have also been calculated as a function of delay time. The final populations of the initial and target states depend on the delay time. For the ladder system, the variation of the delay time has a small effect on the final population of the intermediate state.

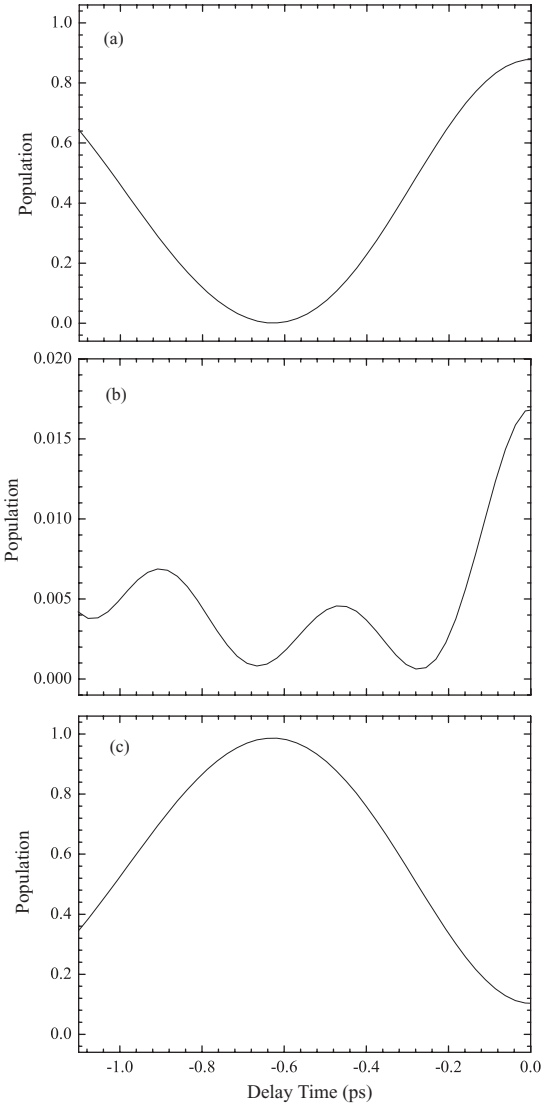

FIG. 7. The final populations at the end of the pulse sequence versus the delay time Δt. (a) The population of the initial state. (b) The population of the intermediate state. (c) The population of the target state. All other parameters are the same as in Fig. 5(e).

ACKNOWLEDGMENTS

This work is supported by the Education Department of Liaoning Province (Grant No. 2009A131).

[1] S. Magnier, M. Persico, and N. Rahman, Phys. Rev. Lett. **83**, 2159 (1999).
[2] E. A. Shapiro, M. Spanner, and M. Y. Ivanov, Phys. Rev. Lett. **91**, 237901 (2003).
[3] B. J. Sussman, D. Townsend, M. Y. Ivanov, and A. Stolow, Science **314**, 278 (2006).
[4] M. V. Korolkov, G. K. Paramonov, and B. Schmidt, J. Chem. Phys. **105**, 1862 (1996).
[5] S. Thomas, S. Guérin, and H. R. Jauslin, Phys. Rev. A **71**, 013402 (2005).
[6] Y.-Y. Niu, S.-M. Wang, and S.-L. Cong, Chem. Phys. Lett. **428**, 7 (2006).
[7] T. Hornung, M. Motzkus, and R. de Vivie-Riedle, Phys. Rev. A **65**, 021403(R) (2002).
[8] S. Shi, A. Woody, and H. Rabitz, J. Chem. Phys. **88**, 6870 (1988).
[9] Y. N. Demkov and V. N. Ostrovsky, Phys. Rev. A **61**, 032705 (2000).
[10] S. Chelkowski, A. D. Bandrauk, and P. B. Corkum, Phys. Rev. Lett. **65**, 2355 (1990).
[11] U. Gaubatz, P. Rudecki, S. Schiemann, and K. Bergmann, J. Chem. Phys. **92**, 5363 (1990).
[12] B. M. Garraway and K. A. Suominen, Phys. Rev. Lett. **80**, 932 (1998).
[13] L. P. Yatsenko, B. W. Shore, T. Halfmann, K. Bergmann, and A. Vardi, Phys. Rev. A **60**, R4237 (1999).
[14] N. V. Vitanov and B. W. Shore, Phys. Rev. A **73**, 053402 (2006).
[15] R. G. Unanyan, B. W. Shore, and K. Bergmann, Phys. Rev. A **59**, 2910 (1999).
[16] H. T. K. Bergmann and B. W. Shore, Rev. Mod. Phys. **70**, 1003 (1998).
[17] C. Marx and W. Jakubetz, J. Chem. Phys. **125**, 234103 (2006).
[18] H. A. Camp, M. H. Shah, M. L. Trachy, O. L. Weaver, and B. D. DePaola, Phys. Rev. A **71**, 053401 (2005).
[19] T. Cubel, B. K. Teo, V. S. Malinovsky, J. R. Guest, A. Reinhard, B. Knuffman, P. R. Berman, and G. Raithel, Phys. Rev. A **72**, 023405 (2005).
[20] M. A. Gearba, H. A. Camp, M. L. Trachy, G. Veshapidze, M. H. Shah, H. U. Jang, and B. D. DePaola, Phys. Rev. A **76**, 013406 (2007).
[21] S.-Y. Meng, L.-B. Fu, and J. Liu, Phys. Rev. A **78**, 053410 (2008).
[22] U. Gaubatz, P. Rudecki, M. Becker, S. Schiemann, M. Külz, and K. Bergmann, Chem. Phys. Lett. **149**, 463 (1988).
[23] F. Remacle and R. D. Levine, Phys. Rev. A **73**, 033820 (2006).
[24] A. Brown, Chem. Phys. **342**, 16 (2007).
[25] S. Gräfe, W. Kiefer, and V. Engel, J. Chem. Phys. **127**, 134306 (2007).
[26] C.-C. Shu, J. Yu, K.-J. Yuan, W.-H. Hu, J. Yang, and S.-L. Cong, Phys. Rev. A **79**, 023418 (2009).
[27] I. V. Andrianov and G. K. Paramonov, Phys. Rev. A **59**, 2134 (1999).
[28] Y.-C. Han, K.-J. Yuan, W.-H. Hu, T.-M. Yan, and S.-L. Cong, J. Chem. Phys. **128**, 134303 (2008).
[29] C. C. Marston and G. G. Balint-Kurti, J. Chem. Phys. **91**, 3571 (1989).
[30] M. D. Feit, J. A. Fleck Jr., and A. Steiger, J. Comput. Phys. **47**, 412 (1982).
[31] D. Kosloff and O. Kosloff, J. Comput. Phys. **52**, 35 (1983).
[32] J. C. Light, I. P. Hamilton, and J. V. Lill, J. Chem. Phys. **82**, 1400 (1985).